# Young's Modulus Variation within Polystyrene Injection Moldings

B. O'DONNELL and J. R. WHITE*

Department of Mechanical, Materials and Manufacturing Engineering, University of Newcastle-upon-Tyne, Newcastle-upon-Tyne, NE1 7RU, United Kingdom

SYNOPSIS

Young's modulus distributions in the depth direction within injection moldings made from polystyrene have been investigated by employing two independent techniques. Both methods show that the material close to the surface exhibits relatively high stiffness, whereas at all other depths a lower uniform stiffness exists. The depth dependency of other material characteristics, such as tan $\delta$ peaks in the dynamic mechanical thermal analysis spectra and molecular orientation, have been investigated in an attempt to correlate them with the stiffness distributions. It appears that the thermomechanical history of the different regions within the moldings, particularly the stresses acting during flow and the temperature gradients set up during cooling, are primarily responsible for the Young's modulus distributions presented here. © 1993 John Wiley & Sons, Inc.

## INTRODUCTION

Several studies have revealed that the properties of the skin and the core of injection moldings are quite different,[1-6] and it is evident that this influences the mechanical and fracture properties of moldings. Differences between skin and core material are present even in glassy polymers, though the extent of the respective regions is sometimes difficult to assess. In the work presented here, the main field of interest was a study of Young's modulus variations within polystyrene moldings. To aid interpretation, it was necessary also to investigate variations in molecular orientation. It is recognized that the properties of the skin material may not be uniform, rather that there will be property gradients across the thickness of the skin, and investigative techniques were sought that are sensitive to such variations. Some of the techniques applied in this investigation have been used to study fiber-reinforced semicrystalline moldings and this will be presented in a future paper.[7]

## EXPERIMENTAL

Injection moldings were produced from BP Chemicals KLP polystyrene using a Butler-Smith 100/60 reciprocating screw machine. The mold cavity had a single end gate and produced straight-bar-shaped moldings. This ensured that the flow was essentially unidirectional. The bars had the following approximate dimensions: length = 190 mm, width = 12.5 mm, and thickness = 3.2 mm. At the beginning of each molding run, at least 20 bars were rejected to ensure that all specimens collected for testing were identical. The molding conditions were chosen to produce visually acceptable moldings, free from sink marks, voids, etc., and were left unaltered during the molding operation. Once the moldings had been labeled and allowed to cool to room temperature, their birefringence patterns were examined, using crossed polars, to quickly check if there were any apparent differences between the moldings. None were found to be present and it was concluded that the moldings were identical.

Three experimental techniques were employed to study these moldings:

- Bend testing allied to a layer-removal technique to determine Young's modulus distributions.

* To whom correspondence should be addressed.

Journal of Applied Polymer Science, Vol. 47, 189–198 (1993)
 CCC 0021-8995/93/020189-10

- Dynamic mechanical thermal analysis.
- The determination of the birefringence distribution to assess molecular orientation.

### Young's Modulus Using Bending Measurements

The variation of Young's modulus in the depth direction was obtained using a procedure based on the three-point bend test. The force deflection relationship of the bars was obtained before thin uniform layers of equal thickness were removed from both faces and the test repeated. This procedure was repeated several times, until the remaining portion was too thin to obtain accurate stiffness measurements in bending. For each bending test, a linear relationship was obtained between the force ($F$) and deflection ($\delta$), and the gradient, $F/\delta$, was used to calculate the function

$$S^*(a) = \frac{Fl^3}{6\delta} \tag{1}$$

where $2l$ is the distance between the two extreme supports. The value of $S^*(a)$ for each of the tests was then plotted vs. $a$, the total thickness removed from each face, and a curve drawn through the data points. The gradient of this plot, $dS^*(a)/da$, was measured at selected values of $a$ and used in the following formula, the derivation of which is given in Appendix 1:

$$E(z_0 - a) = \frac{-1}{2b(z_0 - a)^2} \frac{dS^*(a)}{da} \tag{2}$$

where $b$ is the width of the bar and $2z_0$ is the thickness before layers are removed. $E(z_0 - a)$ is the Young's modulus at the position $z_0 - a$ measured from the central plane.

### Dynamic Mechanical Thermal Analysis

A Polymer Laboratories dynamic mechanical thermal analyser (DMTA) was employed to measure the Young's modulus distribution in the polystyrene injection moldings. This machine is particularly useful for this type of investigation as it enables very thin specimens to be employed (the minimum thickness of the test samples is about 0.2 mm due to geometrical limitations and difficulties associated with sample preparation), thus allowing specific locations within the moldings to be isolated (e.g., the skin layer) and tested. Very short samples can be tested, permitting measurements to be made transverse to the flow direction, which in the bars used here limits the sample length to 12.5 mm. The specimens are tested in double or single cantilever bending while in an enclosed controlled-temperature environment, allowing the storage modulus, $E'$, and tan $\delta$ to be determined over a large range of temperatures. Previous work in this laboratory has shown that the raw stiffness data obtained with this type of machine lack absolute accuracy, but an experimental procedure has been developed that produces results that can be used to obtain reliable qualitative information.[8] More accurate values can be obtained by testing samples of different lengths using different clamping frames and using an extrapolation procedure to eliminate end effects, but this procedure is time-consuming and was not applied here. For the through-thickness modulus profiles, the samples were tested only at room temperature.

Thin samples, between 0.2 and 0.3 mm, were removed from known locations within the moldings using high-speed milling.[9] Each molding could produce several test pieces from a particular depth. Test pieces were cut only from the more central positions along the length of the bars so that modifications to property that might be present near to the gate were avoided. Samples were cut both parallel and perpendicular to the bar axis (major flow direction) and were used to investigate anisotropy in the moldings.

### Birefringence

Birefringence studies are well established as a means of investigating the levels of molecular orientation in glassy polymers.[10-14] In this work, a through-thickness birefringence profile was determined to assess the depth dependency of the molecular orientation.

If birefringence varies with depth (the $z$ direction), then relative retardation for a thin layer thickness $\delta z$ at depth $z$ is

$$\delta R = \Delta n(z)\delta z \tag{3}$$

Total relative retardation for thickness $t$ is then

$$R = \int_0^t \delta R = \int_0^t \Delta n(z)dz \tag{4}$$

Differentiating eq. (4) gives

$$\frac{dR}{dt} = \Delta n(t) \tag{5}$$

where $\Delta n(t)$ is the birefringence at a position $t$. Hence, the first derivative of relative retardation with respect to thickness will represent the inherent birefringence at any point. This procedure was adopted to obtain the birefringence distribution in the thickness direction of injection-molded polystyrene.

## RESULTS

### Young's Modulus Using Bending Measurements

Figure 1 shows a through-thickness Young's modulus distribution obtained using the layer removal and bending test method described above. The results extend only to depths of about 1.3 mm from the surface. This is unavoidable because of difficulties with machining and conducting bend tests on very thin samples ($t \leq 0.6$ mm remains when both sides have been machined to a depth of 1.3 mm). This is not a serious disadvantage here as the DMTA results indicate that the central regions have a fairly uniform stiffness, consistent with the constant birefringence in this region. The values of Young's modulus shown in Figure 1 (about 3 $GN/m^2$) are in close agreement with data obtained from the material supplier.[15] Figure 1 indicates the presence of a skin layer extending to depths of $\approx$ 0.1 mm, wherein exists a very steep stiffness gradient, falling from the surface. There is also an indication of a very slight rise in stiffness centered at a depth of $\approx$ 0.5 mm,[8] the same position at which a small rise in molecular orientation was indicated by the birefringence measurements (see below).

It is recognized that the calculated Young's modulus at the surface might be in error, as at this point the gradient of the $S^*(a)$ vs. $a$ curve is most difficult to measure. Repeat tests on further polystyrene bars[8] all showed the stiffness at the surface to be higher than in the interior of the moldings, though it was difficult to get reproducible values at the surface.

### Dynamic Mechanical Thermal Analysis

DMTA measurements of the through-thickness Young's modulus distribution at room temperature were made using samples 0.2–0.3 mm thick. The values of Young's modulus were lower than those measured by the bending technique, but showed a similar trend with the material close to the surface exhibiting a higher stiffness than that in the interior.

Figure 2 shows typical DMTA traces produced using polystyrene skin samples cut with their long axes, respectively, parallel and perpendicular to the flow direction, whereas Figure 3 shows typical DMTA traces produced using polystyrene core samples also cut parallel and perpendicular to the flow

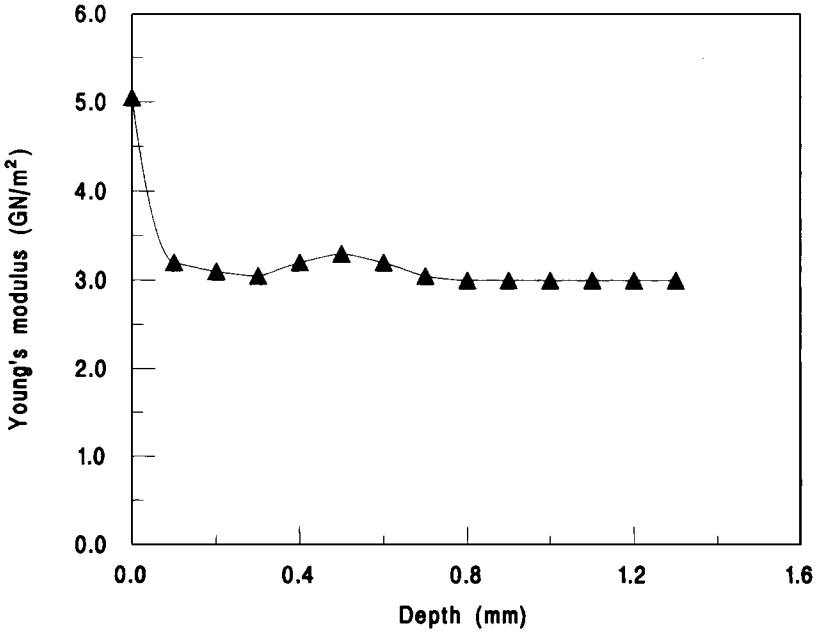


**Figure 1** The depth-dependent distribution of Young's modulus determined for a polystyrene injection molding using the static bending procedure.

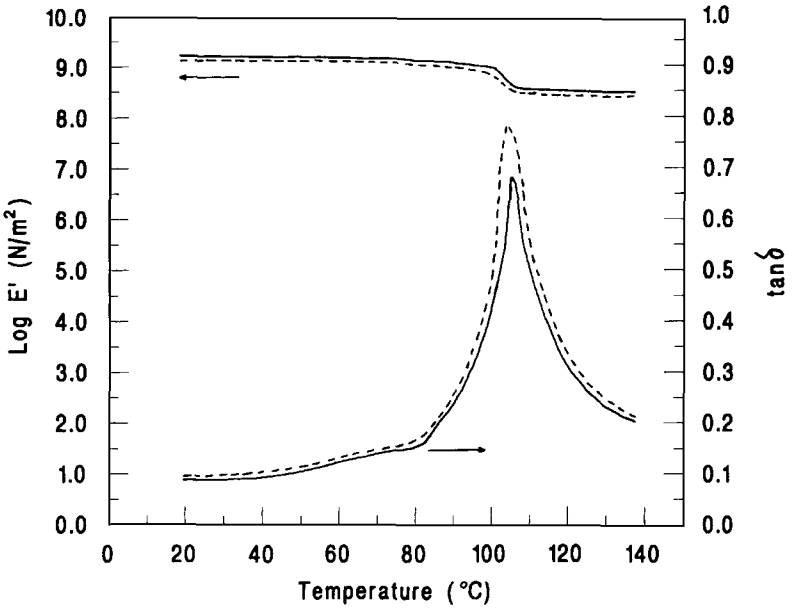


**Figure 2** DMTA traces for polystyrene skin samples: (——) sample cut parallel to MFD; (– – –) sample cut perpendicular to MFD.

direction. Although we have expressed reservations regarding the absolute values of the modulus measurements, the differences shown by the different samples were highly reproducible.

The position of the tan $\delta$ peak is taken to be the glass transition temperature, $T_g$. For the skin samples, $T_g$ is 105°C for both parallel and perpendicular samples, whereas $T_g$ is 103°C for both types of core sample.

The skin stiffness measurement is higher when tests are carried out on samples cut parallel to flow than when cut perpendicular to flow. The same is found with the core material. This suggests the presence of some molecular orientation in the core.

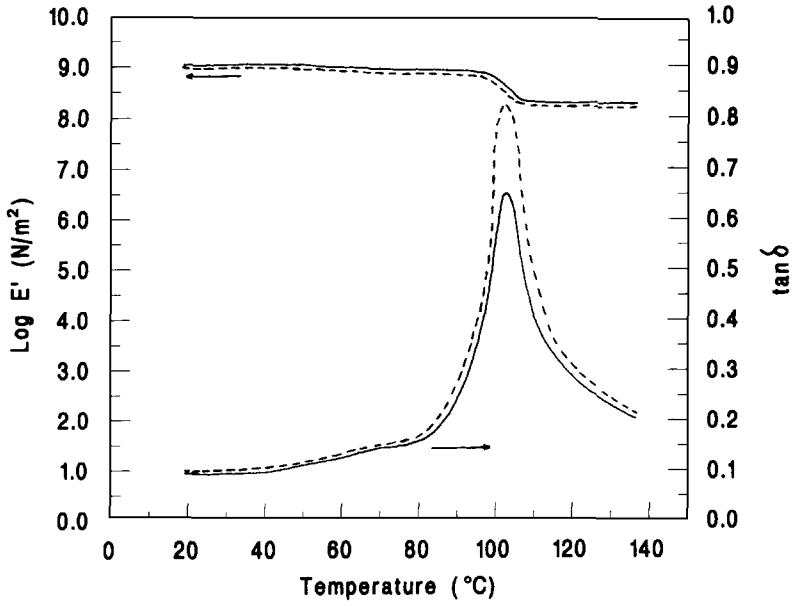


**Figure 3** DMTA traces for polystyrene core samples: (——) sample cut parallel to MFD; (– – –) sample cut perpendicular to MFD.

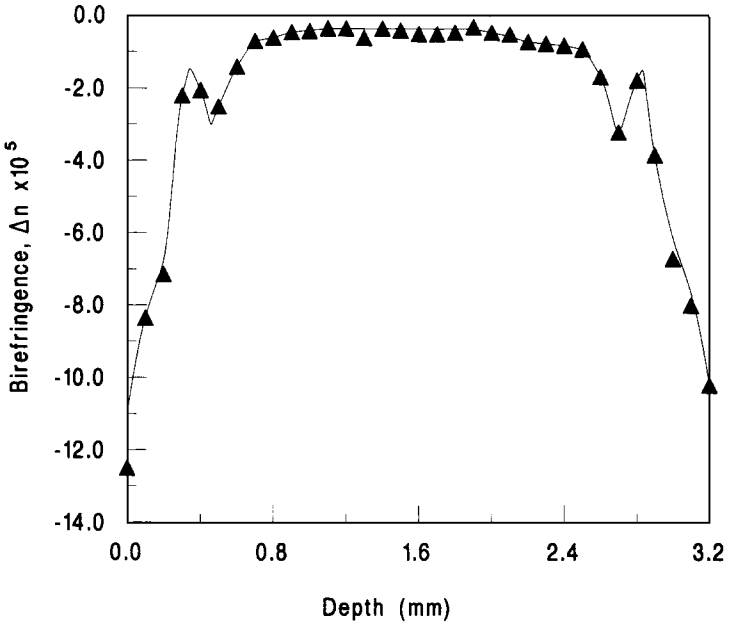


**Figure 4** The depth-dependent distribution of birefringence in the polystyrene injection molding.

There is also a difference in the height of the tan $\delta$ peaks between different samples. Skin and core samples cut parallel to the flow direction show tan $\delta$ peaks of similar height. The same is true with samples cut perpendicular to the flow direction. However, the samples cut perpendicular to flow have tan $\delta$ peaks higher than those obtained with samples cut parallel to flow.

### Birefringence

Figure 4 is the plot of birefringence vs. depth for an injection-molded polystyrene bar. During the layer removal operation it was observed that the molding remained fairly flat, indicating that the residual stress levels in the moldings are fairly low and that the birefringence is essentially an indication of molecular orientation.

The birefringence exhibits reasonably good symmetry about the center of the molding (at $a$ = 1.6 mm) and shows that high levels of molecular alignment exist in the skin, and low levels, in the core. There is also evidence of a localized increase in orientation at locations centered around depths of 0.5 mm. These results indicate that the variations in stiffness measured by the DMTA are probably caused by variations in molecular orientation. This will be discussed further below.

## DISCUSSION

The development of stiffness anisotropy and depth variations within an injection molding arises as a consequence of the stresses that act within the melt during the flow and cooling stages of the molding process. During flow shear and elongational stresses produce preferred molecular orientation, whereas during cooling, the extent of molecular chain relaxations is determined by the rate of cooling.

Publications on the properties of injection moldings often use the terms "skin" and "core," relating, respectively, to the material that solidifies rapidly at the cold mold wall and the material in the interior that cools slowly, allowing molecular relaxations to occur. The skin and core usually have different mechanical and/or morphological characteristics, though the extent of the skin layer is often not measured and the exact differences in property are rarely determined. In injection-molded polystyrene, it is the orientation of the molecular chains that is principally responsible for the stiffness characteristics. Molecular orientation in injection-molded polystyrene has been studied previously by others but has not been related to a detailed stiffness distribution of the type presented here.

The DMTA traces show some important differences between the skin and core material in polystyrene. Skin samples cut parallel to the major flow

direction exhibited a higher stiffness than did the core samples cut in the same direction. This can be attributed to the molecular chains in the skin layer being preferentially oriented parallel to the major flow axis. The origin of this orientation was described by Tadmor.[16] Extensional flow at the melt front induces a high degree of molecular alignment parallel to the major flow direction in the frozen skin layer. At locations further behind the melt front, shear flow dominates and induces molecular orientation parallel to the flow direction in the melt. This distribution of the shear-induced orientation will be modified by molecular relaxations during cooling until the final distribution of molecular orientation in the solid molding is reached.

The presence of high molecular orientation in the skin is seen in the birefringence profile shown in Figure 4 and appears to extend to depths of about 0.3 mm from the surface. However, birefringence in polystyrene may not correlate directly with main chain orientation, but, rather, with phenyl group orientation. Previous work in this laboratory[17] has shown the birefringence in thick polystyrene moldings, measuring 12.7 × 12.7 mm in cross section, to develop primarily during cooling after ejection from the mold. The level of birefringence in these moldings immediately after ejection was low, implying that there was very little flow-induced orientation present and that molecular orientation develops during subsequent solidification as evidenced by the developing birefringence. The most likely source of birefringence arising during solidification is orientation of the phenyl groups, which seems to occur because of their need to pack parallel to one another rather than as a consequence of pronounced molecular backbone extension. The core material contains molecules that show a much lower degree of molecular orientation: first, because the shear rates in the melt are lower at this location, producing a low degree of molecular alignment, and second, because the cooling rate is sufficiently low to allow the molecular chains to take up more random orientations before solidification is complete.

Another difference between the skin and core regions is that of density. Iacopi and White[18] showed that the skin has a higher density than does the core, the difference in the respective densities being dependent on injection pressure. Annealing the moldings was found to remove these differences. It is proposed here that this difference in densities is responsible for the difference in relaxation temperatures between the skin and core. The $T_g$ of the skin material is 105°C, and that of the core, 103°C. The $\alpha$-transition in polystyrene involves motion of the bulky phenyl groups. This is hindered by the high molecular alignment in the skin, especially if the phenyl groups on adjacent molecular chains interlock. Thus, sufficient free volume for the $\alpha$-transition can be attained only when the skin is raised to higher temperatures.

Comparison between the DMTA traces for skin material tested when the sample lengths are, respectively, parallel and perpendicular to the major flow direction show the former to be stiffer and to have a lower tan $\delta$ peak at $T_g$. The higher stiffness can be attributed to molecular orientation. We speculate that the differences in the tan $\delta$ peak heights can be explained by considering the activating forces in relation to the extended molecular chains. If the activating force supplied by the driving mechanism of the DMTA acts parallel to the direction of an extended molecular chain, it cannot assist segmental motion in the chain and this part of the molecule will not contribute to the damping process. If the activating force is acting perpendicular to an extended region of the molecule, then it may assist the relevant motion and contribute to the damping, causing the tan $\delta$ peak to be raised at $T_g$. Similar behavior is found in the core, and we speculate that the residual molecular orientation causes this effect even though it is not as pronounced as in the skin.

Comparison of the DMTA traces for the skin and core samples tested with their lengths perpendicular to the major flow direction shows the skin to be stiffer and to have a higher $T_g$ (by about 2°C). The differences in $T_g$ have been explained previously using free-volume considerations. The difference in stiffness is the reverse of that expected from molecular orientation considerations. The core material, having a more random molecular orientation, would be expected to be stiffer than the skin when measured in the transverse-to-flow direction. However, there is also a difference in density between the skin and core, and it appears that the higher density of the skin impairs relative molecular chain movement sufficiently to maintain a high stiffness perpendicular to the flow direction, higher than that in the lower-density core.

The through-thickness stiffness profiles obtained by the bend test analysis yields further information about differences between the skin and core regions in the polystyrene moldings. The most significant feature of the bend test stiffness profiles is the distribution of the stiffness in the skin. In a semicrystalline polymer, the skin thickness can be easily determined from morphological observations. However, this cannot be done with amorphous glassy polymers and the extent of the skin in these mate-

rials must be assessed by other methods, if, indeed, the term "skin" can be applied to such materials. The stiffness profiles suggest that the skin extends to a depth of about 0.1 mm and that within this depth there is a very rapid decrease in stiffness from the surface. The birefringence profile shows that the molecular orientation parallel to the flow direction similarly decreases very rapidly in this region. However, it should be noted from the birefringence profile that a high extent of frozen-in molecular orientation exists to depths of about 0.3 mm. This demonstrates the difficulty that exists in accurately determining the thickness of the skin, though this study suggests a value less than or equal to 0.3 mm. Recall also that the value of the stiffness at the surface is difficult to determine accurately, though repeated tests suggest a value some 100–200% greater than that in the core. The Young's modulus in the interior is shown to be uniform, at about 3 $GN/m^2$.

The birefringence profile also shows an increase in molecular orientation centered at depths of 0.5 mm in from each surface. This behavior has been observed previously in injection-molded polystyrene[14] and has been attributed to a local rise in shear flow at these locations. As the increase in molecular orientation at these depths appears to be significant in comparison to the orientation in the central region of the bar, it might be expected to produce a corresponding increase in stiffness. The birefringence at a depth of 0.5 mm is about $-3 \times 10^{-5}$, the same as at depths of 0.3 mm. The stiffness has already leveled out at 3 $GN/m^2$ at 0.3 mm from the surface so that any rise in stiffness at depths of $\approx$ 0.5 mm is not expected to be large. This is seen in Figure 1, where there is, nevertheless, some evidence of a very small increase in stiffness at this position.

It appears from this work that the distribution of stiffness in the polystyrene injection moldings arises as a consequence of the flow behavior of the melt and the different rates of cooling experienced at different locations within the solidifying melt. The Young's modulus at any location within the molding depends on the orientation and the density of the material and varies according to the direction in which it is measured. It follows that the distribution of stiffness can be significantly affected by a suitable heat treatment. Changes in the molding parameters will also modify the stiffness distribution. It has already been shown that changing the injection pressure affects the difference in density between the skin and core.[18] Increasing the temperature of the mold will decrease the thermal gradients present during cooling and allow more molecular relaxation to occur. These and other methods can be employed to reduce the difference in property between the skin and core regions. Conversely, these differences can be enhanced by appropriate changes in the processing conditions.

Hoare and Hull[19] indicated that the crazing stresses within a polystyrene molding are dependent upon the direction of the applied stress relative to any molecular orientation and on the type of orientation. However, the crazing stresses could be further modified if high shear stresses arise within a molding when loaded, caused by the difference in stiffness between adjacent layers. Previously, the control of the site of fracture initiation has been attributed partly to the level of residual stresses,[20] but we have not found discussion of the effects of stiffness variations in the literature.

Finally, Figure 5 shows the resultant stress distribution in a polystyrene molding at the point of fracture after a tensile strain of 1.25% has been applied. This corresponds to a tensile strength of 45 $MN/m^2$ for the molding. This curve was obtained using the cumulative effects of the stiffness distribution in Figure 1 and a typical residual stress distribution for a polystyrene molding processed under similar conditions[21] (Fig. 6). As can be seen, the tensile stresses in the surface regions are considerably higher than those in the core even though the surface regions are in compression when no external strain is applied. It is in these surface layers that we would expect fracture to be initiated from a craze.

## CONCLUSIONS

A method of determining the Young's modulus as a function of depth in a polymer molding has been developed based upon a layer-removal technique and a three-point bend test. The technique has yielded highly reproducible results for polystyrene moldings and has been shown to be sensitive to changes in stiffness caused by molecular alignment. However, it must be remembered that this analysis applies only to a symmetrical molding with a centrally located neutral plane. Young's modulus profiles obtained using this technique have identified the presence of two distinct regions in the polystyrene moldings. There is an extensive central region of uniform stiffness and a layer close to the surface wherein exists a sharp stiffness gradient. This layer has been found to extend to depths of about 0.1 mm, though, morphologically, it appears no different from the rest of the molding.

The distribution of molecular orientation in the polystyrene moldings indicates that the stiffness

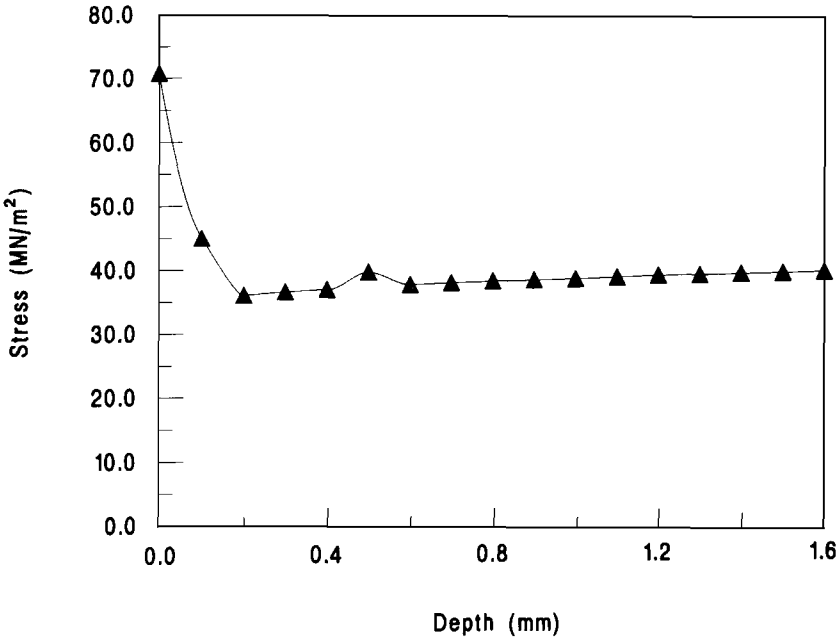


**Figure 5** The distribution of stress in a polystyrene molding when a tensile strain of 1.25% is applied.

distribution arises primarily as a consequence of molecular alignment, though the DMTA measurements also suggest that a contribution from material density is present. A high degree of molecular alignment has been found in the polymer close to the surface of the molding. The birefringence profile has identified the presence of a local increase in molecular alignment at depths of about 0.5 mm in the moldings, and there is some evidence to suggest that this causes a corresponding small increase in stiffness at the same depths, though this has not been proved conclusively.

The authors would like to thank Natraj Bead Manufacturing Company, India, for providing funding for this work.

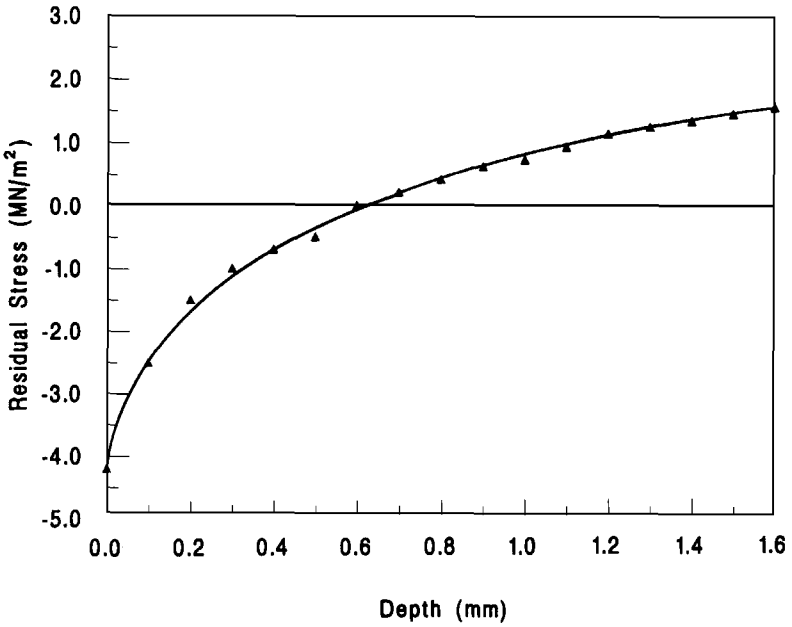


**Figure 6** The residual stress distribution in a polystyrene molding (after Haworth[21]).

## APPENDIX

The following analysis and experimental procedure were developed for the measurement of Young's modulus profiles through the depth of injection-molded bars. Figure A.1 shows a diagrammatic representation of an injection-molded bar.

The neutral plane, i.e., the plane that experiences no strain when the bar is bent, is assumed to be centrally located, as shown. The upper and lower surfaces of the bar are at a distance $z_0$ above and below the neutral plane, respectively. If equal layers of material of thickness $a$ are removed from the top and bottom surfaces of the bar, then the two new surfaces created will lie at a distance of $z_0 - a$ from the neutral plane.

In this analysis, it is assumed that the distribution of the Young's modulus in the depth direction is symmetrical about the neutral plane. Consider now the case when the injection-molded bar is subjected to a three-point bend test as shown in Figure A.2, using a span of $l$ between the central point of load application and the supports.

The internal bending moment when the bar is bent to a radius $R$ is given by

$$M(a, R, x) = \int_{-z_0+a}^{z_0-a} \frac{bz^2E(z)dz}{R(x)} = \frac{1}{R(x)} \int_{-z_0+a}^{z_0-a} bz^2E(z)dz \quad \text{(A.1)}$$

where $b$ is the width of the bar.

Let

$$S^*(a) = \int_{-z_0+a}^{z_0-a} bz^2E(z)dz \quad \text{(A.2)}$$

Therefore,

$$M(a, R, x) = \frac{S^*(a)}{R(x)} \quad \text{(A.3)}$$

Consider a point A in the bar. When the bar is bent, let $x$ and $z$ be the horizontal and vertical coordinates of the point A.

The radius of curvature at A is given by

$$\frac{1}{R(x)} = \frac{\frac{d^2z}{dx^2}}{\left[1 + \left(\frac{dz}{dx}\right)^2\right]^{3/2}} \quad \text{(A.4)}$$

In practice, the value of $dz/dx$ is small and $(dz)/(dx)^2 \ll 1$.

Therefore,

$$\frac{1}{R(x)} = \frac{d^2z}{dx^2} \quad \text{(A.5)}$$

The bending moment produced by a force $W$ acting at a distance $x$ from the midpoint of the bar is given by

$$M(a, R, x) = W(l - x) \quad \text{(A.6)}$$

Combining eqs. (A.3), (A.5), and (A.6) gives

$$S^*(a)\frac{d^2z}{dx^2} = W(l - x) \quad \text{(A.7)}$$

Integration of eq. (A.7) gives

$$S^*(a)\frac{dz}{dx} = W(l - x) + C_1 \quad \text{(A.8)}$$

When $x = 0$, $dz/dx = 0$, giving $C_1 = 0$.

Integration of eq. (A.8) gives

$$S^*(a)z = W\left(\frac{lx^2}{2} - \frac{x^3}{6}\right) + C_2 \quad \text{(A.9)}$$

When $x = 0$, $z = 0$, giving $C_2 = 0$.

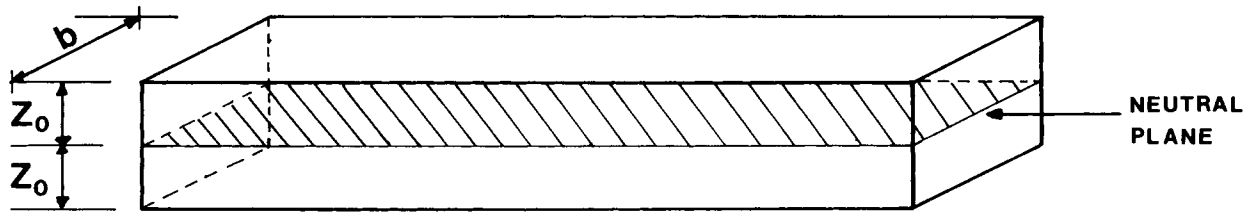


**Figure A.1** Diagrammatic representation of an injection molding.

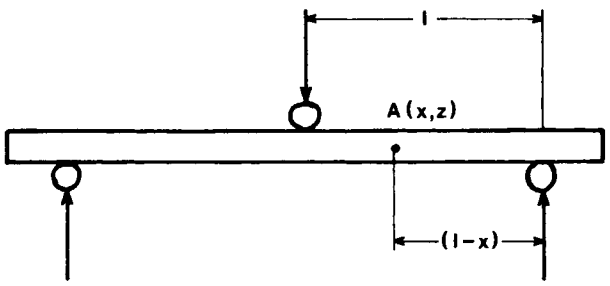


**Figure A.2** The three-point bend test geometry.

When $x = l$, $z$ = deflection, $\delta$, and $W = F/2$, so that

$$S^*(a) = \frac{Fl^3}{6\delta} \qquad \text{(A.10)}$$

It is possible to determine values of $S^*(a)$ experimentally, via simple three-point bend tests, and, hence, the relationship between $S^*(a)$ and the depth removed, $a$, can be determined.

Now

$$S^*(a) = \int_{-z_0+a}^{z_0-a} bz^2E(z)dz \qquad \text{(A.11)}$$

Therefore,

$$\frac{dS^*(a)}{da} = \frac{d}{da}\left[\int_{-z_0+a}^{z_0-a} bz^2E(z)dz\right]$$

If, as we assume, $E(z)$ is an even function [i.e., $E(z) = E(-z)$], this equation can be written as

$$\frac{dS^*(a)}{da} = \frac{d}{da}\left[2\int_0^{z_0-a} bz^2E(z)dz\right]$$

Let $q = z_0 - a$. Hence, $dq = -da$. Therefore,

$$\frac{dS^*(a)}{da} = \frac{-d}{dq}\left[2\int_0^q bz^2E(z)dz\right] = -2bq^2E(q)$$

i.e.,

$$\frac{dS^*(a)}{da} = -2b(z_0 - a)^2E(z_0 - a)$$

or

$$E(z_0 - a) = \frac{-1}{2b(z_0 - a)^2}\frac{dS^*(a)}{da} \qquad \text{(A.12)}$$

where $E(z_0 - a)$ is the Young's modulus of the injection-molded bar at a distance of $(z_0 - a)$ from the neutral plane.

Values for $dS^*(a)/da$ are obtained by measuring gradients at selected values of $a$ from a plot of $S^*(a)$ vs. $a$ determined from bend tests. Values of $E(z_0 - a)$ can therefore be calculated from the above equation and a plot of $E(z_0 - a)$ vs. depth, $a$, can be obtained. In this way, a profile of the Young's modulus of the injection-molded bar in the depth direction can be determined.

## REFERENCES

1. M. Fujiyama, *Kobunshi Ronbunshu,* **32,** 411 (1975) [English ed., **4,** 534 (1975).]
2. M. Fujiyama and S. Kimura, *Kobunshi Ronbunshu,* **32,** 581 (1975) [English ed., **4,** 764 (1975)].
3. M. Fujiyama and S. Kimura, *Kobunshi Ronbunshu,* **32,** 591 (1975) [English ed., **4,** 777 (1975)].
4. M. Fujiyama and S. Kimura, *J. Appl. Polym. Sci.,* **22,** 1225 (1978).
5. M. R. Kamal and F. H. Moy, *Chem. Eng. Commun.,* **12,** 253 (1981).
6. M. R. Kamal and F. H. Moy, *Polym. Eng. Rev.,* **2,** 381 (1983).
7. B. O'Donnell and J. R. White, to appear.
8. B. O'Donnell, PhD Thesis, University of Newcastle upon Tyne, 1990.
9. M. W. A. Paterson, PhD Thesis, University of Newcastle upon Tyne, 1990.
10. R. L. Ballman and H. L. Toor, *Mod. Plast.,* **38,** 113 (1960).
11. Z. Bakerdjian and M. R. Kamal, *Polym. Eng. Sci.,* **17,** 96 (1977).
12. W. Dietz, J. L. White, and E. S. Clark, *Polym. Eng. Sci.,* **18,** 273 (1978).
13. M. R. Kamal and V. Tan, *Polym. Eng. Sci.,* **19,** 558 (1979).
14. B. E. Read, J. C. Duncan, and D. E. Meyer, *Polym. Test.,* **4,** 143 (1984).
15. BP Chemicals, Technical Data.
16. Z. Tadmor, *J. Appl. Polym. Sci.,* **18,** 1753 (1974).
17. B. O'Donnell, M. W. A. Paterson, and J. R. White, unpublished results.
18. A. V. Iacopi and J. R. White, *J. Appl. Polym. Sci.,* **33,** 577 (1987).
19. L. Hoare and D. Hull, *Polym. Eng. Sci.,* **17,** 204 (1977).
20. A. Siegmann, A. Buchman, and S. Kenig, *Polym. Eng. Sci.,* **21,** 997 (1981).
21. B. Haworth, MSc Thesis, University of Newcastle upon Tyne, 1979.

*Received October 18, 1991*
*Accepted March 2, 1992*